Running head: Turanose mediated WOX5 expression rescues *cre1*

***Author for correspondence:**

Maitrayee DasGupta

Address: Department of Biochemistry, University of Calcutta,

35, Ballygunge Circular Road, Kolkata-700019, West Bengal, India

Phone No. +91-33-2475-4680; Fax: +91-33-2476-4419

Email ID: maitrayee_d@hotmail.com

Journal Research area:

Signalling and response

Turanose mediated *WOX5* expression rescues symbiosis in cytokinin perception mutant *cre1*

Anindya Kundu[1,2], Firoz Molla[1] and Maitrayee DasGupta[1*]

[1] Department of Biochemistry, University of Calcutta, Kolkata 700019, India

One sentence summary:

Sugar signalling rescues symbiosis in *Medicago truncatula* cytokinin perception mutant *cre1*

Keywords:

Cytokinin signalling, Sugar signalling, turanose, WOX5, root nodule symbiosis

58 **Footnotes**

59

60 *Address correspondence to maitrayee_d@hotmail.com

61 **Author contribution:**

62 A.K. M.D., conceived the idea; A.K. and F.M. performed experiments and analysed the data.

63 A.K. and M.D wrote the paper. All authors read and approved the final manuscript.

64

65 **Financial support:**

66 This work was funded by Grants from Govt. of India: DST (DST EMR/2015/001006).

67 Fellowship to A.K (Council of Scientific and Industrial Research, CSIR-09/028[0756]/2009–

68 EMR–I) and fellowship to F.M (University Grant Commission, No.F.16-6(DEC.2016)/2017

69 (NET).UGC Ref no- 771

70

71 [2]**Present address:** NIAB EMR, Kent, UK

72

73 The authors declare no conflict of interest.

74

75

76

77

78

79

80

81

82

83

84

85

86

ABSTRACT

Rhizobia-legume interaction recruits cytokinin for the induction of nodule primordia in the cortex. In *Medicago truncatula*, cytokinin signalling involves flavonoid mediated local alteration of polar auxin transport for triggering cortical cell division. Since sugar signalling is widely evidenced to trigger auxin responses, we explored whether sugar treatment could compensate for cytokinin signalling in *M. truncatula* cytokinin perception mutant *cre1*. Herein we demonstrate that turanose, a non-metabolizable sucrose analogue can trigger auxin response and show signs of recovery of symbiosis in *cre1*. Additionally, turanose upregulated the expression of WUSCHEL-related homeobox 5 (*MtWOX5*) which prompted us to check if overexpression of WOX5 could rescue *cre1*. Intriguingly, while overexpression of *MtWOX5* failed, WOX5 from *Arachis hypogaea* (*AhWOX5*) completely restored functional symbiosis in *cre1* with an efficiency resembling the wildtype. This indicate that indeterminate and determinate WOX5 responds to differential cues for nodule development and is consistent with their distinct clustering in distance trees. The mechanism of compensation of cytokinin signalling for recovery of symbiosis in *cre1* was distinct for turanose treatment and *AhWOX5* expression. Turanose increased *MtHK2* level by ~5-fold and doubled the level of *MtRR4* whereas *AhWOX5* elevated the level of *MtRR4* by ~12-fold without affecting the level of *MtHK2/3*. Thus, turanose compensated MtCRE1 at receptor level whereas WOX5 restored the signalling at the level of response regulators. We propose a working model to discuss how sugar mediated WOX5 signalling have compensated MtCRE1 to recover normal progress of symbiosis *in cre1*.

INTRODUCTION

In root nodule symbiosis (RNS) rhizobia-legume interaction activates the SYM pathway which in turn activates cytokinin response for the induction of a *de novo* meristem in the root cortical cells (Frugier et al., 2008). Cytokinin-signaling causes local auxin accumulation at the site of incipient nodule primordia by modulating the expression of auxin transporters (Plet et al., 2011; Ng et al., 2015). These phytohormonal signals and the SYM pathway together reprogram the cortical cells and regulate their division, ultimately building a nodule primordium for the endocytic accommodation of the symbionts (Mathesius et al., 2000; Suzaki et al., 2012).

Several evidences projected the hierarchical organization of the Nod factor-dependent activation of SYM-Pathway and cytokinin signalling pathway (Frugier et al., 2008). For example, Nod factor induced accumulation of cytokinin by upregulation of several cytokinin biosynthesis genes indicates its precedence to cytokinin signalling (Held et al., 2014; Van Zeijl et al., 2015). This explains why majority of Nod factor-induced transcriptional changes were absent in Cytokinin Perception Mutant *cre1* in *M. truncatula* (Van Zeijl et al., 2015). Genetic evidences further confirm this hierarchy, when constitutive activation of CCaMK (*snf1*) fails to trigger spontaneous nodulation in absence of cytokinin signalling in *cre1* whereas constitutive activation of cytokinin receptor LHK1 (*snf2*) triggered nodulation in *dmi2* (Madsen et al., 2010). Cytokinin oxidase/dehydrogenase expressed during nodule development restricts the level of active cytokinin for balancing its positive role in nodule organogenesis with its negative effect on rhizobial infection at the root epidermis (Reid et al., 2016). Therefore, apart from being the key endogenous signal for nodule development and differentiation (Plet et al., 2011; Kundu and DASGupta, 2018), cytokinin also maintains the homeostasis of the symbiotic interaction indicating that the *SYM* pathway and cytokinin signaling are connected through feedback loops (Miri et al., 2016).

Hierarchically auxin is projected to act next to cytokinin during nodule development (Plet et al., 2011; Suzaki et al., 2012). Several evidences indicated directional transport and local accumulation of auxin to be important for the development of nodule primordia and accordingly application of auxin transport inhibitors is sufficient to induce nodule-like cell division (Rightmyer and Long, 2011; Ng et al., 2015). Accumulation of auxin could be either due to regulation of its transport or biosynthesis and cytokinin is known to regulate both these processes (Van Noorden et al., 2006; Pernisová et al., 2009; Jones et al., 2010). The response

regulators (RRs), functioning downstream to cytokinin receptors modulate auxin signaling via SHY2 mediated downregulation of auxin transporters (Dello Ioio et al., 2008; Moubayidin et al., 2010). Recent evidence revealed that cytokinin controls flavonoid concentration in roots and local application of flavonoid could recover no dulation in the cytokinin perception mutant *cre1* mutant of *M. truncatula* (Ng et al., 2015). Intriguingly, auxin transport inhibitors can cause pseudonodule formation in SYM pathway mutants like *nsp2* and *nin* that function downstream of cytokinin signalling further indicating that auxin accumulation and response could be the final call for initiation of cortical cell division during RNS (Rightmyer and Long, 2011).

Sugars play a role in plant development and several evidences indicate a crosstalk between sugar signalling and auxin responses. For example, (i) there are mutants that are commonly resistant to both sugar and auxin responses (Ohto et al., 2006), (ii) auxin biosynthetic genes are modulated by sugar status (Leclere et al., 2010; Sairanen et al., 2013) and (iii) there is a connection between polar auxin transport and sugar metabolism (Stokes et al., 2013). Moreover, sugar signalling is also responsible for specific developmental responses like trehalose mediated inhibition of root elongation and glucose affecting root architecture through auxin-based signal transduction (Wingler et al., 2000; Mishra et al., 2009). Sugar signalling is also connected with auxin response of the conserved WUS (WUSCHEL)/WOX (WUSCHEL-related homeobox gene)-CLV regulatory system that are involved in meristem maintenance. For example, WOX9 is typically required for auxin response in Shoot Apical meristem (SAM) and sucrose can compensate for loss of WOX9*(stip)*, that arrests growth soon after germination (Xuelin Wu, Tsagaye Dabi, 2005). Also, the expression of WOX5, which maintains localized auxin maxima in the root apical meristem (RAM) is induced by auxin and turanose, a non-metabolizable sucrose analogue (Gonzali et al., 2005).

CRE1(CYTOKININ RESPONSE1), an orthologue of AHK4, is a membrane-bound cytokinin receptor necessary for nodulation in *M. truncatula* (Gonzalez-Rizzo et al., 2006; Plet et al., 2011). Earlier reports indicated that the *M. truncatula cre1* mutant is defective in auxin accumulation in the root cortex following *S. meliloti* inoculation (Ng et al., 2015). A plausible hypothesis could be that sugar signalling would rescue cytokinin perception mutant *cre1* by inducing auxin responses. Sucrose is an important metabolite transported to nodules and sucrose transporters are upregulated with rhizobial infection but their specific role in signalling during nodule development is still oblivious (Lalonde et al., 2004; Ayre, 2011). Turanose, a nonmetabolizable analogue of sucrose provides an opportunity to study its role as

a signalling molecule (Sinha et al., 2002). Herein we show that turanose treatment upregulates auxin responses and successfully rescues the nodulation efficiency in *cre1*. Turanose treatment induced the expression of WOX5 which is in consistence with earlier reports demonstrating that WOX5 functions downstream to auxin signalling for the initiation of nodule primordia (Chen et al., 2009; Osipova et al., 2012). Finally, we demonstrated that WOX5 overexpression can rescue *cre1*with an efficiency resembling the wildtype but were intrigued to find that only *AhWOX5* from *Arachis hypogaea* (determinate) but not *MtWOX5* (indeterminate) could do so. This indicated WOX5 from indeterminate and determinate legume responds differential cues for their functional activation. A working hypothesis is proposed based on our observations on how turanose treatment and WOX5 expression could have compensated MtCRE1 for restoring symbiosis in *cre1*.

RESULTS

Turanose rescues nodulation in cytokinin perception mutant *cre1*

Based on several evidences that highlight the crosstalk between sugar signalling and auxin responses we wanted to explore whether sugar signalling could rescue rhizobial symbiosis in cytokinin perception mutant *cre1* (Leclere et al., 2010; Ljung et al., 2015). For this we used turanose, a nonmetabolizable sucrose which is previously reported to trigger auxin response (Gonzali et al., 2005). Both *A17* and *cre1* roots were grown on plates with 10^{-2}M or 10^{-3}M of turanose for 1 week before being infected with *Sinorhizobium meliloti Sm2011-pBHR-mRFP*. Turanose treatment did not have any significant effect on root and shoot length and the lateral root number in either *A17* or *cre1* plants (Supplementary Fig. 1). The effect on nodule development was significant where 10^{-3}M Turanose provided the best efficacy in nodule formation in *cre1* and therefore was used in all later experiments. At 4WAI, there were ~1.4 ± 0.9 nodules in untreated *cre1* roots whereas turanose treatment resulted in formation of ~12 ± 3.3 nodules per plant (Fig 1a). Almost 42% of the turanose rescued nodules in *cre1* were pink functional nodules, with proper colonization and differentiation of bacteroids (Fig. 1a-c). In the rest of the nodules that were nonfunctional and whitish, rhizobia were mostly trapped in the nodule apex (Fig1b) or entrapped in cortical infection threads (Fig1c). As compared to *cre1*, nodulation was much higher in A17 plants. On an average turanose untreated A17 plants produced ~21 ± 2.9 nodules by 3WAI which increased to ~28 ± 8.7 nodules upon turanose treatment without any significant change in the number of functional nodules. The increase in nodule number in A17/turanose is primarily because of significant increase in

merged white nodules where rhizobia were entrapped in infection threads in the infection zone (Fig 1c). It may be noted that formation of merged nodules is a common feature in turanose treated *cre1* and A17 roots indicating that turanose induced loss of spatial distribution is independent of CRE1 mediated cytokinin signalling. This higher number of merged nodules can be explained by higher auxin concentration that led to increased cortical cell division as previously reported for supernodulating mutant of *Medicago sunn-4* where such disorder in spatial distribution pattern was noted (Schnabel et al., 2005; Van Noorden et al., 2006).

Turanose treatment triggered cytokinin and auxin responses and induced *WOX5* expression in *cre1*

For the readout of cytokinin and auxin signalling, *A17* and *cre1* roots were transformed with *pTCS:GUS* (Fig.2a-f) and *pDR5:GUS* (Fig.2g-l) respectively (Suzaki et al., 2012; Breakspear et al., 2014; Ng et al., 2015). The transgenic roots were treated with 10^{-3}M turanose for 1 week before scoring the read out using untreated roots and infected roots at 1WAI as reference. In untreated A17 and *cre1* roots *pTCS:GUS* expression was barely detectable and was strictly restricted to root tips (Fig.2a and d). Turanose treatment significantly enhanced *pTCS:GUS* expression in both A17 and *cre1* roots and in both cases the expression was spread in the root hair zone (Fig.2b and e). The infected *cre1* roots were in complete contrast where cytokinin response was significantly lower and restricted to root tips as compared to the turanose treated *cre1* roots or the infected *A17* roots (Fig.2c, e and f).This absence of cytokinin response in infected *cre1* roots explains the symbiotic inefficiency of this mutant whereas the increase in cytokinin response in presence of turanose explains the rescue of nodulation in *cre1*. Expression of *pDR5:GUS* was low in untreated A17 roots which barely increased upon turanose treatment and in both cases, expression was restricted within root tips and vascular bundles (Fig. 2g-h). In untreated *cre1*, expression of *pDR5:GUS* was also low and primarily restricted to root tips (Fig.2j). In contrast to these cases, turanose treated *cre1* roots had a significant increase in *pDR5:GUS* expression throughout the root system indicating MtCRE1 to antagonise the sugar mediated auxin response (Fig. 2k). In infected A17 roots the auxin response was significantly higher than the corresponding turanose treated roots which is in complete contrast with *cre1* roots where auxin response was significantly lower in infected roots as compared to the turanose treated roots (Fig.2i and l). This absence of auxin response in infected *cre1* roots explains the

symbiotic inefficiency of this mutant whereas the increase in auxin response in presence of turanose explains the rescue of nodulation in *cre1*.

Earlier reports indicated that auxin treatment upregulated *MtWOX5* expression and there is significant increase in expression of *MtWOX5* transcription factor during nodulation in *M. truncatula* roots (Gonzali et al., 2005; Chen et al., 2009; Osipova et al., 2012). Additionally, (Gonzali et al., 2005) demonstrated that turanose can induce *AtWOX5* expression through an auxin mediated pathway in *Arabidopsis*. We checked whether elevated auxin response in turanose treated *cre1*roots was accompanied with upregulation of expression of *MtWOX5*. For this we monitored the level of *pWOX5:GUS* expression after turanose treatment and used untreated roots and infected roots at 1WAI as reference. Expression of *MtWOX5* in untreated roots of A17 was very low whereas in *cre1* it was relatively higher (Fig.2m, p and Supplementary Fig. 2). In both cases expression of *pWOX5:GUS* was primarily restricted to root tips though in *cre1* it was diffused throughout the root system indicating MtCRE1 to have a role in restricting the expression of *MtWOX5*. Upon turanose treatment *pWOX5:GUS* expression significantly increased in both A17 and *cre1* and the expression was spread in the entire root system (Fig.2n and q, Supplementary fig.2). In both cases expression of *pWOX5-GUS* was higher in infected as compared to uninfected roots but was significantly lower than turanose treated roots (Fig.2o and r). The correlation between auxin response and *MtWOX5* expression was distinct in A17 and *cre1* roots. In turanose treated A17 roots lower auxin response was coupled with higher *MtWOX5* expression whereas in turanose treated *cre1* roots the expanded expression of *pWOX5:GUS* correlated well with ectopic up-regulation of *pDR5:GUS* signals. On the other hand, in infected A17 and *cre1* roots auxin responses correlates well with *pWOX5:GUS* expression where responses were higher in A17 and lower in *cre1*.

WOX5 from *Arachis hypogaea* (*AhWOX5*) rescues nodulation in cytokinin perception mutant *cre1*

The significant increase in WOX5 expression in turanose treated *cre1* roots raises the question whether overexpression of a single homeodomain transcription factor like WOX5 would rescue the symbiotic phenotypes in *cre1*. Phylogenetically WOX5 from determinate nodule forming legumes like *Arachis hypogaea*, *Glycine max*, *Vigna angularis*, *Cajanus cajan* and *Phaseolus vulgaris* sand indeterminate nodulators like *Cicer arietinum*, *Pisum*

sativum, *Medicago truncatula* and *Trifolium subterraneum* distinctly clusters in a distance tree and therefore could be amenable to distinct regulations (Supplementary fig. 3). Recent evidences indicate that auxin and cytokinin signalling are differentially regulated depending upon the nodule ontogeny (Ng and Mathesius, 2018). While acropetal auxin transport inhibition is essential for indeterminate nodule development, it is dispensable for determinate nodulation. We therefore attempted to rescue cre1 by overexpressing *MtWOX5* and *AhWOX5* from a determinate legume like *Arachis hypogaea*. *Mt*WOX5 is 86% similar to *Ah*WOX5 and the homeobox domain is highly conserved with 96% similarity (Supplementary fig. 3).

Full length *MtWOX5* and *AhWOX5* was amplified from cDNA prepared from respective plant roots. *Mt*WOX5 codes for a protein of 184aa (XP_003616581.1) and *Ah*WOX5 codes for a protein of 215aa (KT820790). Transformed roots of *cre1* overexpressing *MtWOX5* and *AhWOX5* were inoculated with *S. meliloti Sm2011-pBHR-mRFP* and *Sm1021-pXLGD4-lacZ* (Fig.3a-d). Infection threads were detectable within 2-3WAI in both vector transformed and *MtWOX5* overexpressed *cre1* roots but almost all of them were abandoned in the root hair or epidermis (Fig.3a-b). In both cases cortical cell division was noted but these primordia like structures remain uninfected (Fig.3a). On the other hand, within 2WAI, overexpression of *AhWOX5* resulted in formation of ~10 normal ITs per root system (Fig.3a-b). The normal ITs progressed towards the subtending nodule primordia generated in the cortex to ensure proper rhizobial accommodation. In accordance with the abnormal progression of ITs there was no improvement of nodulation efficiency in *MtWOX5* overexpressing *cre1* roots even at 6WAI (n=10). But overexpression of *AhWOX5* lead to significant nodulation in *cre1* roots by 4WAI where the total number of nodules was comparable to wild type A17 roots (Fig.3c). Almost 75% of these nodules were pink and could reduce acetylene and ultrastructure analysis revealed them to have properly differentiated bacteroids (Fig.3f-g). Rest of the nodules that were whitish, resembled the nodules formed in *cre1* or *MtWOX5* overexpressed *cre1* where bacteria were either trapped inside infection threads in the nodule apex or were trapped within a network of infection threads in the infection zone (Fig.3g). The level of expression of WOX5 in *MtWOX5* and *AhWOX5* overexpressed *cre1* roots were comparable indicating that MtWOX5 requires further functional cues to become functional in *cre1* (Fig.3e). Since overexpression of neither *AhWOX5* nor *MtWOX5* had any effect in nodule number or their organisation in A17, it is clear that their signalling output is under the homeostatic control of a large network of fate governing factors.

Effect of turanose treatment and *AhWOX5* overexpression on cytokinin signalling during recovery of symbiosis in *cre1*

To understand how cytokinin signalling was compensated for the recovery of symbiosis we checked the expression of cytokinin signalling components in turanose treated and *AhWOX5* overexpressed nodulated roots of *cre1*. First, we checked the expression of other paralogous of *MtCRE1* like *MtHK2* and *MtHK3*. It was noted earlier that the late and inefficient nodule development in *cre1* is due to the redundant involvement of receptors MtHK2 and MtHK3 (Held et al., 2014; Boivin et al., 2016). Intriguingly, in turanose treated A17 roots expression of both these receptors increased by ~20-fold (Fig.4a-c) demonstrating a direct involvement of sugar signalling in cytokinin response. Upon turanose treatment in *cre1*, expression of *MtHK2* increased by ~5-fold without any notable increase in *MtHK3* indicating a role of MtCRE1 in regulating the sugar signalling mediated expression of *MtHK3*. The increased expression of *MtHK2* appeared to compensate for *MtCRE1* in the receptor level and explained the restoration of symbiosis in *cre1*. In contrast to turanose treatment where *MtHK2* and *MtHK3* expression was upregulated, their expression was unaffected in presence of *AhWOX5* in both A17 and *cre1* roots. This suggests the mechanism of compensation of MtCRE1 by *AhWOX5* overexpression must be downstream.

Downstream to cytokinin receptors, a histidyl-aspartyl multistep phosphorelay is initiated, leading to the expression of Type-A RRs as primary response genes. Several type-A RRs such as *MtRR4*, *MtRR8* and *MtRR9* are induced during nodulation and coordinate the downstream functional responses (Gonzalez-Rizzo et al., 2006; Tirichine et al., 2007; Op den Camp et al., 2011). We therefore checked the expression of these Type-A RRs in nodulated roots of turanose treated and *AhWOX5* overexpressed *cre1* and *A17* (Fig.4d-f). In turanose treated A17 roots, where *MtHK2/3* expression was ~20-fold higher, the level of *MtRR4* just doubled whereas in *AhWOX5* overexpressed roots where *MtHK2/3* expression was significantly low, *MtRR4* level still increased by ~1.5-fold indicating that the expression of *MtRR4* may not be a perfect readout for the level of *MtHK2* and *MtHK3* (Fig.4d). In *cre1*, the intrinsic expression of *MtRR4* was lower than A17. Intriguingly, in *AhWOX5* overexpressed *cre1* roots where symbiosis was perfectly restored the level of *MtRR4* increased by ~15-fold which was at least 3 fold more than the level of *MtRR4* in A17. In turanose treated *cre1* roots where symbiosis was partially restored the level of *MtRR4* just doubled. Level of *MtRR8* and *MtRR9* either significantly decreased or remained unchanged in both A17 and *cre1* in both turanose treated and *AhWOX5* overexpressed conditions indicating that they may not have

any role in restoration of symbiosis in *cre1* (Fig.4e-f). Finally, in tune to successful recovery of symbiosis in *cre1* in presence of turanose or overexpressed *AhWOX5*, the expression of symbiosis markers like *MtSYMREM*, *MtIPD3*, *MtNIN*, and *MtENOD40* was restored to the level of A17 under symbiotic conditions (Fig.4g-j).

DISCUSSION

The symbiotic inefficiency in *cre1* is due to its inability to induce flavonoids that regulate auxin transport for reactivation of cortical cells (Ng et al., 2015). In accordance, treatment with flavonoids allowed auxin transport control and rescued nodulation efficiency in *cre1*. Herein we demonstrate that (i) turanose significantly induces both cytokinin and auxin response in *cre1* and rescues symbiosis (Fig.1). While sugar signalling is known to control several distinct aspects of plant development our results for the first time show its role in nodule development. (ii) Turanose induced auxin response was significantly higher in *cre1* as compared to A17 indicating a cytokinin dependent link between sugar status and auxin response (Fig.2). This observation highlights an antagonistic interaction between CRE1 mediated cytokinin signalling and sugar signalling as noted before (Moore et al., 2003). Finally, (iii) we show that turanose induces the expression of WOX5, a marker of meristem maintenance (Sarkar et al., 2007). Overexpression of this single homeodomain transcription factor could completely restore functional symbiosis in *cre1* without affecting the expression level of *MtHK2* & *MtHK3* (Fig.3-4), suggesting WOX5 to function downstream to CRE1 as observed in SAM. These observations are summarised in a working model and discussed in the backdrop of our present understanding about cytokinin signalling during nodule initiation (Fig.5).

Sucrose metabolism is highly responsive to both internal and external environmental signals and can in turn dramatically alter plant development (Koch, 2004). In general, hexoses favor cell division and expansion, whereas sucrose favour differentiation and maturation (Ã et al., 2003; Borisjuk et al., 2003). Several evidences indicate a connection between sucrose signalling and the conserved WOX-CLV regulatory system that are involved in meristem maintenance (Francis and Halford, 2006). The best example is the loss of WOX9 mutant *stip*, that has SAM defects and arrests growth soon after germination. Remarkably, *stip* could be rescued by sucrose, and thus a gene that is typically required for normal meristem development was compensated by sugar signalling (Xuelin Wu, Tsagaye Dabi, 2005).

Additionally, cytokinins are required for *STIP* (WOX9) expression, linking cytokinin signalling to meristem establishment through the action of STIP (Skylar et al., 2010). Another example is FANTASTIC FOUR (FAF4) protein that control meristem size through WUS proteins. FAF4 overexpression arrests root growth shortly after germination and the aberration can be rescued by addition of exogenous sucrose (Wahl et al., 2010). Additional examples involve turanose-treated *Arabidopsis* seedlings that are characterized by short primary root. Turanose-insensitive mutant was a loss-of-function mutant of WOX5 and turanose insensitivity was associated with constitutive activation of IAA conjugation. This demonstrated a direct link with WOX signalling and sugar status and indicated WOX5 to be a positive trigger for free IAA availability (Gonzali et al., 2005). In summary, all these examples clearly demonstrate that sucrose signals overlap phytohormonal signals and their crosstalk is then directly sensed by the WOX group of transcription factors for regulating plant development. Herein, our observations demonstrate how turanose signalling induces auxin mediated WOX5 expression to recover a complex phenotype like root nodule symbiosis in a cytokinin receptor mutant, pointing to a deep conservation of signalling for developing and sustenance of meristems (Fig.1-2). We indicate this sugar and auxin mediated WOX5 expression to be functionally parallel to the MtCRE1 mediated signalling (Fig.5).

WOX genes are common regulators of cell proliferation and differentiation and are part of a subnetwork of cell fate-governing factors (Richards et al., 2015). The common mode of action for WOX proteins is prevention of premature differentiation by transcriptional repression that maintains the stem cell niche in meristems which is also conserved in the nodule meristem (Sarkar et al., 2007). The complete rescue of symbiosis in *cre1* by *AhWOX5* was intriguing because ectopic expression of WOX5, a mobile organizer signal that represses differentiation, was expected to maintain stemness and restrict organogenesis. It may be noted that overexpression of WOX5 had no effect on nodulation efficiency in A17 which again suggests that WOX5 is tightly controlled by the fate governing signalling network at post transcriptional level (Fig.5). We were further intrigued by the fact that *AhWOX5* from a determinate legume but not the intrinsic *MtWOX5* could restore symbiosis in *cre1* where the reverse was expected (Fig.3d). This sharp difference between MtWOX5 and AhWOX5 could be because they were differentially responsive to post transcriptional and post translational regulations. The indeterminate and determinate WOX5 were distinctly clustered in a distance tree (Supplementary fig.3) and one important difference between them was in the WUS box motif which is TL**Q**LFP in AhWOX5 and TL**E**LFP in MtWOX5. Since WUS box is the major

417 determinant of biological action of WOX proteins and is essential for both activation and
418 repression function of this transcription factor (Ikeda et al., 2009; Dolzblasz et al., 2016), the
419 difference in charge in this motif could be a significant determinant of the contrasting
420 outcome. In response to external cues WOX proteins transiently turn to activator mode for
421 triggering differentiation during plant development (Forzani et al., 2014). To explain the
422 sharp difference between *MtWOX5* and *AhWOX5* in their ability to restore symbiosis in *cre1*
423 we hypothesize *MtWOX5* to be trapped in its default mode of repression whereas *AhWOX5*
424 can override the control. Such differences between indeterminate and determinate WOX5
425 may also have a role in determining the perpetual and terminated meristems in respective
426 legumes.

427 The importance of auxin signalling in WOX5 mediated restoration of symbiotic efficiency in
428 *cre1* (Fig.2) is in accordance with the following evidences: (i) Both in *Arabidopsis* as well as
429 in *Medicago* auxin induces WOX5 expression in roots (Gonzali et al., 2005; Osipova et al.,
430 2012). (ii) Induction of WOX5 by turanose results in repression of SUR2, a modulator of
431 auxin homeostasis, resulting in a marked increase in free IAA content. (iii)WOX5 directly
432 modulates expression of auxin biosynthetic genes and thus provides a robust mechanism for
433 the maintenance of auxin response maximum (Tian et al., 2014). Thus, unlike flavonoids that
434 regulate auxin gradients by affecting its transport, WOX5 expression regulate auxin response
435 through its synthesis and conjugation. Recent evidence in recruitment of auxin biosynthesis
436 gene YUCCA2 and YUCCA8 during nodule development further highlight the important role
437 of auxin biosynthesis during nodule development (Schiessl et al., 2019). It may be noted that
438 incidence of merged nodules which is an indication of higher auxin concentration was only
439 noted in presence of turanose and not WOX5 overexpressed roots indicating WOX5
440 expression to keep auxin under homeostatic control. The increased auxin response in *cre1* as
441 compared to A17 highlighted the reciprocity in sugar and MtCRE1 signalling (Fig.2). Similar
442 reciprocity between cytokinin and sugar signalling was noted earlier where plants with
443 impaired cytokinin receptors CRE1 and AHK3 display increased sugar sensitivity and
444 decreased sensitivity to sugar in HXK1 mutant was accompanied with increased cytokinin
445 response (Moore et al., 2003; Franco-zorrilla et al., 2005). It is apparent that a bidirectional
446 antagonistic interaction operates between sugars and CRE1 mediated cytokinin signalling in
447 generating auxin response (Fig.5).

448 The point is how MtCRE1 dependent cytokinin signalling is compensated by turanose
449 mediated WOX5 expression in *cre1*. The late and inefficient nodule development in *cre1* is

due to the redundant involvement of receptors MtHK2 and MtHK3 (Held et al., 2014; Boivin et al., 2016). In presence of turanose there was a significant upregulation of *MtHK2* which can serve as a proxy for CRE1 and explain the rescue of symbiosis in *cre1* (Fig.4). On the other hand, *AhWOX5* overexpression did not affect the expression of any of the HKs in A17 as well as *cre1* indicating the mechanism of WOX5 mediated restoration of symbiosis in *cre1* to be certainly downstream. WOX proteins has been shown to directly repress the transcription of several Type-A RRs genes, which encode negative regulators of cytokinin signalling (Zhao et al., 2009).We found *MtRR8* to be repressed and *MtRR9* to be unaffected in presence of turanose as well as *AhWOX5* (Fig.4). Intriguingly, we found that expression of *MtRR4* that gets induced in presence of rhizobia (Plet et al., 2011) was doubled in presence of turanose in both A17 and *cre1* and its expression was ~12 times more in presence of *AhWOX5* in *cre1* roots. The increased expression of *MtRR4* may serve as a proxy for cytokinin signalling in *cre1* for developing symbiosis (Fig.5). Again, in contrast to negative activity of several of the type-A ARRs, ARR4 has also been shown to have positive interactions (To et al., 2007). Since the efficacy of restoration of symbiosis with *AhWOX5* expression is much higher than what we observed with turanose we presume the pathway of restoration by *AhWOX5* to evade all upstream feed-back homeostatic loops (Fig.4).

In a working model (Fig.5) we propose sugar signalling to restore symbiosis in *cre1* by (i) redundant action of MtHK2 that compensates MtCRE1 and by (ii) directly triggering auxin responses (Blue arrows). *AhWOX5* do not trigger *MtHK2/3* expression and is proposed to restore symbiosis by induction of (i) *MtRR4* a response regulator required for symbiosis and by directly triggering auxin responses (Red arrows). Since overexpression of WOX5 do not trigger cortical cell division in *cre1*, the trigger of SYM pathway is essential for WOX5 action. Also, since overexpression of *AhWOX5* has no effect on nodule organogenesis in A17, WOX5 function appear to be governed by post transcriptional homeostatic controls. This layout can now serve as model for understanding the role of sugar signalling mediated auxin response in RNS and help elucidate the regulation of indeterminate and a determinate WOX5.

MATERIALS AND METHODS

Plant and Rhizobial strains

Medicago cre1 seeds (Plet et al., 2011), *Agrobacterium rhizogenes* strain MSU440 and *Sinorhizobium meliloti Sm2011-pBHR-mRFP* and *Sm1021-pXLGD4-lacZ* (Boivin et al., 1990) strain were used.

Constructs

Full length MtWOX5 and AhWOX5 are amplified from cDNA prepared from nodulated roots of *Medicago truncatula* and *Arachis hypogaea* (Kundu and DASGupta, 2018) with primers 5'-ATGGAAGAGAGCATGTCAGG-3' and 5'-ACTTACGGTTGAGTTTTGTGTAA-3' (*MtWOX5*) 5'-CACCATGCAGACGGTCCGAGATCTGTC-3' and 5'-CCTTCGCTTAAGTTTCATGTAA-3' (*AhWOX5*) and cloned into pENTER-dTOPO (Invitrogen). The entry clones are recombined through LR clonase Gateway technology (Invitrogen) into pK7WGF2 to generate 35S::eGFP-MtWOX5 and 35S::eGFP-AhWOX5. pDR5:GUS, pWOX5:GUS and pTCS:GUS were obtained from (Franssen et al., 2015).

Turanose treatment

Plants are germinated as previously described Saha et. al.,2014 followed by their transfer into Fahraeus medium containing different concentration of Turanose: 10^{-3}M and 10^{-2}M. For promoter assay plants are maintained for 2-3 weeks in Turanose plates before harvesting and staining. For nodulation assay plants are inoculated in the plates with *Sm2011-pBHR-mRFP*/ *Sm1021-pXLGD4-lacZ* grown overnight at 28ºC in YM to OD600=1.0 and then diluted 1:50 in half-strength B&D (Broughton and Dilworth, 1971). Nodulation is scored 3-4WAI.

Phenotypic analysis

Generation of composite *M. truncatula* plants and scoring nodulation, phenotypic analysis and confocal microscopy were performed as described previously (Saha et al., 2014).

For detailed description of methods pertaining to growth condition, phenotypic assay, microscopy, qRT-PCR and primers used see Supplemental Methods S1.

ACKNOWLEDGEMENT

We thank Florian Frugier for *cre1* seeds, Henk J. Franssen for providing us with *pDR:GUS*, *pTCS:GUS* and *pWOX5:GUS* constructs, Ton Bisseling & Erik Limpens for *S. meliloti* harbouring *pBHR-mRFP*, Douglas R. Cook for *Agrobacterium* strain MSU440.

SUPPLEMENTAL DATA

Supplementary Materials and Methods

Supplementary Table 1: List of qRT-PCR primers

Supplementary figure 1: Root morphology of A17 and *cre1* under different concentration of Turanose

Supplementary figure 2: Relative expression of *MtWOX5* after turanose treatment

Supplementary figure 3: Sequence alignment and phylogenetic tree of legume WOX5

FIGURE LEGENDS

Figure 1: Complementation of nodulation in *cre1* mutants using non-metabolizable sucrose analogue Turanose. (A) Box plot represents nodule number per plant where histogram represent mean ± SD. Separate plots indicates cumulative and red/white nodules 3-4 weeks after infection (WAI) with *Sinorhizobium meliloti Sm2011-pBHR-mRFP* under control and 10^{-3}M turanose treatment. Student's t-test was used to assess significant differences, where **** and * indicate P<0.0001 and <0.01 respectively, n indicates the number of roots systems with infection events per total number of scored roots.
(B) Morphology of nodules in A17 and *cre1* mutants 3-4WAI. Representative micrograph of control and turanose treated roots indicated as bright field and bright field+ mRFP merged.
(C) Ultrastructure analysis of nodules in A17 and *cre1* after turanose treatment, where the perforated box represents the infection zone with its corresponding enlarged view below the respective images. Total number of each type of nodules observed out of the total observed nodules are indicated at the left-hand corner. (upper panel) Brightfield + mRFP merged and (lower panel) mRFP. Scale bar: B= 500µm, C (upper panel) = 100µm and (lower panel) = 10µm.

Figure 2: Turanose treatment and infection with *Sm2011-pBHR-mRFP* differentially induces cytokinin (*pTCS:GUS*), auxin (*pDR5:GUS*) and WOX5 (*pWOX5:GUS*) expression in A17 and *cre1* mutants. (A-F) *pTCS:GUS* expression in (A-C) A17 roots under control (A), 10^{-3}M Turanose treatment (B) and after *Sm2011* infection (C); (D-F) *cre1* roots under control (D), 10^{-3}M Turanose treatment (E) and after *Sm2011* infection (F).

(G-L) *pDR5:GUS* expression in (G-I) A17 roots under control (G), 10^{-3}M Turanose treatment (H) and after *Sm2011* infection (I); (J-L) *cre1* roots under control (J), 10^{-3}M Turanose treatment (K) and after *Sm2011* infection (L).

(M-R) *pWOX5:GUS* expression in (M-O) A17 roots under control (M), 10^{-3}M Turanose treatment (N) and after *Sm2011* infection (O); in (P-R) *cre1* roots under control (P), 10^{-3}M Turanose treatment (Q) and after *Sm2011* infection.

Root were harvested 1 week post treatment with turanose and 1 week after infection with *Sm2011-pBHR-mRFP*. At least 20 individual samples were observed for each treatment and representative images are presented. Scale bar = 5mm (whole root) and 2mm (single root).

Figure 3: Complementation of nodulation in hairy-root transformed *cre1* mutants by ectopic expression of *AhWOX5*. (A) Epidermal infection thread (IT) observed under bright field microscope 2WAI with *Sm1021-pXLGD4-lacZ* in *cre1* roots transformed with empty vector, *p35S:eGFP-MtWOX5* and *p35S:eGFP-AhWOX5*. Total number of each type of infection threads (IT) observed out of the total number of early infection events are indicated at the left-hand corner. Scale bar = 100µm.

Box plot represents (B) IT/ root system and (C) Nodule number/ root system where histogram represent mean ± SD. Student's t-test was used to assess significant differences, where **** and ** indicates P<0.0001 and P<0.004 respectively and n indicates the number of roots systems with infection events per total number of scored roots.

(D) Morphology of nodules in transgenic hairy-roots of *cre1*mutant 4WAI with *Sm2011-pBHR-mRFP*. Representative micrograph of transgenic roots indicated as bright field+ mRFP merged and inset as eGFP+ mRFP merged and bright field. Scale bar = 1mm and inset = 500µm.

(E) qRT-PCR analysis of *MtWOX5* and *AhWOX5* relative to control transformed (*cre1*) roots normalised against *MtActin*. (F) Acetylene reduction assay (nmole C_2H_4/h/mg nodule) in indicated root system. For E and F, Histogram represents an average of three biological replicates each having n>4 plants and error bar represents SD. Student's t- test was used to assess significant differences, where **** indicate P<0.0001.

(G) Ultrastructure of nodules developed in *cre1* mutant transformed with different constructs where the perforated box represents the infection zone with its corresponding enlarged view below the respective images. Scale bar: G (upper panel) = 100µm and (lower panel) = 10µm. Arrow indicate infection thread and * indicate cell division.

Figure 4: Differential recruitment of cytokinin signalling and sym pathway during the complementation of *cre1* mutant under turanose treatment and *AhWOX5* ectopic expression. qRT-PCR analysis of *MtCRE1* (A), *MtHK2* (B), *MtHK3* (C), *MtRR4* (D), *MtRR8* (E) *MtRR9* (F) *MtSYMREM* (G), *MtIPD3* (H), *MtNIN* (I) and *MtENOD40* (J) 4WAI with *Sm2011-pBHR-mRFP* in roots of A17, A17/Turanose, A17::35S:*AhWOX5*, *cre1*, *cre1*/Turanose and *cre1*::35S:*AhWOX5* relative to A17. *MtActin* was used as a reference gene. Histogram represents an average of three biological replicates each having n>4 plants and error bar represents SD. Student's t-test was used to assess significant differences where ****, ***, ** and * indicate P<0.0001, 0.0001, 0.005 and 0.04 respectively.

Figure 5: Proposed Model for the role of sugar signalling and *WOX5* expression in restoration of symbiotic efficiency in *M. truncatula* cytokinin perception mutant *cre1*. Black arrows indicate the known sym pathway dependent CRE1 activation that leads to auxin accumulation and WOX5 induction to generate the nodule primordia. We propose sugar signalling to restore symbiosis in *cre1* by (i) redundant action of MtHK2 that compensates MtCRE1 and by (ii) directly triggering auxin responses that is inhibited by CRE1 (Blue arrows). WOX5 restore symbiosis in cre1 by induction of (i) *MtRR4* a response regulator required for symbiosis and by directly triggering auxin responses). WOX5 is activated by SYM pathway and its function is governed by post transcriptional homeostatic controls (Red arrows). Forward arrow indicates activation and blunt arrow indicates inactivation.

REFERENCES

Ã WW, Panitz R, Gubatz S, Wang Q, Radchuk R, Weber H, Wobus U (2003) Weschke 2003 - Invertase and transporter control sugar rate during development - protocol dna.pdf. 395–411

Ayre BG (2011) Membrane-transport systems for sucrose in relation to whole-plant carbon partitioning. Mol Plant **4**: 377–394

Boivin C, Camut S, Malpica CA, Truchet G, Rosenberg C (1990) Rhízobíum me/í/otí. 2:

Boivin S, Kazmierczak T, Brault M, Wen J, Gamas P, Mysore KS, Frugier F (2016) Different cytokinin histidine kinase receptors regulate nodule initiation as well as later nodule developmental stages in Medicago truncatula. Plant Cell Environ **39**: 2198–2209

Borisjuk L, Rolletschek H, Wobus U, Weber H (2003) Differentiation of legume cotyledons as related to metabolic gradients and assimilate transport into seeds. J Exp Bot **54**: 503–512

Breakspear A, Liu C, Roy S, Stacey N, Rogers C, Trick M, Morieri G, Mysore KS, Wen J, Oldroyd GED, et al (2014) The root hair "infectome" of medicago truncatula uncovers changes in cell cycle genes and reveals a requirement for auxin signaling in rhizobial infectionw. Plant Cell **26**: 4680–4701

Broughton WJ, Dilworth MJ (1971) Control of leghaemoglobin synthesis in snake beans. Biochem J **125**: 1075–1080

Chen SK, Kurdyukov S, Kereszt A, Wang XD, Gresshoff PM, Rose RJ (2009) The association of homeobox gene expression with stem cell formation and morphogenesis in cultured medicago truncatula. Planta **230**: 827–840

Dolzblasz A, Nardmann J, Clerici E, Causier B, van der Graaff E, Chen J, Davies B, Werr W, Laux T (2016) Stem Cell Regulation by Arabidopsis WOX Genes. Mol Plant **9**: 1028–1039

Forzani C, Aichinger E, Sornay E, Willemsen V, Laux T, Dewitte W, Murray JAH (2014) WOX5 suppresses CYCLIN D activity to establish quiescence at the Center of the root stem cell niche. Curr Biol **24**: 1939–1944

Francis D, Halford NG (2006) Nutrient sensing in plant meristems. Plant Mol Biol **60**: 981–993

Franco-zorrilla M, Martı AC, Leyva A, Paz-ares J (2005) Interaction between Phosphate-Starvation, Sugar, and Cytokinin Signaling in Arabidopsis and the Roles of Cytokinin Receptors CRE1/AHK4 and AHK3. **138**: 847–857

Franssen HJ, Xiao TT, Kulikova O, Wan X, Bisseling T, Scheres B, Heidstra R (2015) Root developmental programs shape the Medicago truncatula nodule meristem. Dev **142**: 2941–2950

Frugier F, Kosuta S, Murray JD, Crespi M, Szczyglowski K (2008) Cytokinin: secret

agent of symbiosis. Trends Plant Sci **13**: 115–120

Gonzalez-Rizzo S, Crespi M, Frugier F (2006) The Medicago truncatula CRE1 cytokinin receptor regulates lateral root development and early symbiotic interaction with Sinorhizobium meliloti. Plant Cell **18**: 2680–2693

Gonzali S, Novi G, Loreti E, Paolicchi F, Poggi A, Alpi A, Perata P (2005) A turanose-insensitive mutant suggests a role for WOX5 in auxin homeostasis in Arabidopsis thaliana. Plant J **44**: 633–645

Held M, Hou H, Miri M, Huynh C, Ross L, Hossain MS, Sato S, Tabata S, Perry J, Wang TL, et al (2014) Lotus japonicus cytokinin receptors work partially redundantly to mediate nodule formation. Plant Cell **26**: 678–694

Ikeda M, Mitsuda N, Ohme-Takagi M (2009) Arabidopsis wuschel is a bifunctional transcription factor that acts as a repressor in stem cell regulation and as an activator in floral patterning. Plant Cell **21**: 3493–3505

Dello Ioio R, Nakamura K, Moubayidin L, Perilli S, Taniguchi M, Morita MT, Aoyama T, Costantino P, Sabatini S (2008) A genetic framework for the control of cell division and differentiation in the root meristem. Science (80-) **322**: 1380–1384

Jones B, Ljung K, Gunnerås SA, Petersson S V., Tarkowski P, Graham N, May S, Dolezal K, Sandberg G (2010) Cytokinin regulation of auxin synthesis in Arabidopsis involves a homeostatic feedback loop regulated via auxin and cytokinin signal transduction. Plant Cell **22**: 2956–2969

Koch K (2004) Sucrose metabolism: Regulatory mechanisms and pivotal roles in sugar sensing and plant development. Curr Opin Plant Biol **7**: 235–246

Kundu A, DASGupta M (2018) Silencing of putative cytokinin receptor histidine kinasel inhibits both inception and differentiation of root nodules in arachis hypogaea. Mol Plant-Microbe Interact **31**: 187–199

Lalonde S, Wipf D, Frommer WB (2004) Transport Mechanisms for Organic Forms of Carbon and Nitrogen Between Source and Sink. Annu Rev Plant Biol **55**: 341–372

Leclere S, Schmelz EA, Chourey PS (2010) Sugar levels regulate tryptophan-dependent auxin biosynthesis in developing maize kernels. Plant Physiol **153**: 306–318

668 **Ljung K, Nemhauser JL, Perata P** (2015) New mechanistic links between sugar and
669 hormone signalling networks. Curr Opin Plant Biol **25**: 130–137

670 **Madsen LH, Tirichine L, Jurkiewicz A, Sullivan JT, Heckmann AB, Bek AS, Ronson**
671 **CW, James EK, Stougaard J** (2010) The molecular network governing nodule
672 organogenesis and infection in the model legume Lotus japonicus. Nat Commun. doi:
673 10.1038/ncomms1009

674 **Mathesius U, Weinman JJ, Rolfe BG, Djordjevic MA** (2000) Rhizobia can induce nodules
675 in white clover by "hijacking" mature cortical cells activated during lateral root
676 development. Mol Plant-Microbe Interact **13**: 170–182

677 **Miri M, Janakirama P, Held M, Ross L, Szczyglowski K** (2016) Into the Root: How
678 Cytokinin Controls Rhizobial Infection. Trends Plant Sci **21**: 178–186

679 **Mishra BS, Singh M, Aggrawal P, Laxmi A** (2009) Glucose and auxin signaling interaction
680 in controlling arabidopsis thaliana seedlings root growth and development. PLoS One.
681 doi: 10.1371/journal.pone.0004502

682 **Moore B, Zhou L, Rolland F, Hall Q, Cheng WH, Liu YX, Hwang I, Jones T, Sheen J**
683 (2003) Role of the Arabidopsis glucose sensor HXK1 in nutrient, light, and hormonal
684 signaling. Science (80-) **300**: 332–336

685 **Moubayidin L, Perilli S, Dello Ioio R, Di Mambro R, Costantino P, Sabatini S** (2010)
686 The rate of cell differentiation controls the arabidopsis root meristem growth phase. Curr
687 Biol **20**: 1138–1143

688 **Ng JLP, Hassan S, Truong TT, Hocart CH, Laffont C, Frugier F, Mathesiusa U** (2015)
689 Flavonoids and auxin transport inhibitors rescue symbiotic nodulation in the Medicago
690 truncatula cytokinin perception mutant cre1. Plant Cell. doi: 10.1105/tpc.15.00231

691 **Ng JLP, Mathesius U** (2018) Acropetal auxin transport inhibition is involved in
692 indeterminate but not determinate nodule formation. Front Plant Sci **9**: 1–13

693 **Van Noorden GE, Ross JJ, Reid JB, Rolfe BG, Mathesius U** (2006) Defective long-
694 distance auxin transport regulation in the Medicago truncatula super numeric nodules
695 mutant. Plant Physiol **140**: 1494–1506

696 **Ohto MA, Hayashi S, Sawa S, Hashimoto-Ohta A, Nakamura K** (2006) Involvement of
697 HLS1 in sugar and auxin signaling in Arabidopsis leaves. Plant Cell Physiol **47**: 1603–

1611

Op den Camp RHM, de Mita S, Lillo A, Cao Q, Limpens E, Bisseling T, Geurts R (2011) A phylogenetic strategy based on a legume-specific whole genome duplication yields symbiotic cytokinin type-A response regulators. Plant Physiol **157**: 2013–2022

Osipova MA, Mortier V, Demchenko KN, Tsyganov VE, Tikhonovich IA, Lutova LA, Dolgikh EA, Goormachtig S (2012) WUSCHEL-RELATED HOMEOBOX5 gene expression and interaction of cle peptides with components of the systemic control add two pieces to the puzzle of autoregulation of nodulation. Plant Physiol **158**: 1329–1341

Pernisová M, Klíma P, Horák J, Válková M, Malbeck J, Souček P, Reichman P, Hoyerová K, Dubová J, Friml J, et al (2009) Cytokinins modulate auxin-induced organogenesis in plants via regulation of the auxin efflux. Proc Natl Acad Sci U S A **106**: 3609–3614

Plet J, Wasson A, Ariel F, Le Signor C, Baker D, Mathesius U, Crespi M, Frugier F (2011) MtCRE1-dependent cytokinin signaling integrates bacterial and plant cues to coordinate symbiotic nodule organogenesis in Medicago truncatula. Plant J **65**: 622–633

Reid DE, Heckmann AB, Novák O, Kelly S, Stougaard J (2016) CYTOKININ OXIDASE/DEHYDROGENASE3 maintains cytokinin homeostasis during root and nodule development in Lotus Japonicus. Plant Physiol **170**: 1060–1074

Richards S, Wink RH, Simon R (2015) Mathematical modelling of WOX5-and CLE40-mediated columella stem cell homeostasis in Arabidopsis. J Exp Bot **66**: 5375–5384

Rightmyer AP, Long SR (2011) Pseudonodule formation by wild-type and symbiotic mutant Medicago truncatula in response to auxin transport inhibitors. Mol Plant-Microbe Interact **24**: 1372–1384

Saha S, Dutta A, Bhattacharya A, DasGupta M (2014) Intracellular catalytic domain of symbiosis receptor kinase hyperactivates spontaneous nodulation in absence of rhizobia. Plant Physiol **166**: 1699–1708

Sairanen I, Novák O, Pěnčík A, Ikeda Y, Jones B, Sandberg G, Ljung K (2013) Soluble carbohydrates regulate auxin biosynthesis via PIF proteins in arabidopsis. Plant Cell **24**: 4907–4916

Sarkar AK, Luijten M, Miyashima S, Lenhard M, Hashimoto T, Nakajima K, Scheres

B, Heidstra R, Laux T (2007) Conserved factors regulate signalling in Arabidopsis thaliana shoot and root stem cell organizers. Nature **446**: 811–814

Schiessl K, Lilley JLS, Lee T, Ahnert S, Grieneisen VA, Oldroyd GED, Schiessl K, Lilley JLS, Lee T, Tamvakis I, et al (2019) Article NODULE INCEPTION Recruits the Lateral Root Developmental Program for Symbiotic Nodule Organogenesis in Medicago truncatula Article NODULE INCEPTION Recruits the Lateral Root Developmental Program for Symbiotic Nodule Organogenesis in Medicago trun. Curr Biol 1–12

Schnabel E, Journet EP, De Carvalho-Niebel F, Duc G, Frugoli J (2005) The Medicago truncatula SUNN gene encodes a CLV1-like leucine-rich repeat receptor kinase that regulates nodule number and root length. Plant Mol Biol **58**: 809–822

Sinha AK, Hofmann MG, Römer U, Köckenberger W, Elling L, Roitsch T (2002) Metabolizable and non-metabolizable sugars activate different signal transduction pathways in tomato. Plant Physiol **128**: 1480–1489

Skylar A, Hong F, Chory J, Weigel D, Wu X (2010) STIMPY mediates cytokinin signaling during shoot meristem establishment in Arabidopsis seedlings. Development **137**: 541–549

Stokes ME, Chattopadhyay A, Wilkins O, Nambara E, Campbell MM (2013) Interplay between sucrose and folate modulates auxin signaling in Arabidopsis. Plant Physiol **162**: 1552–1565

Suzaki T, Yano K, Ito M, Umehara Y, Suganuma N, Kawaguchi M (2012) Positive and negative regulation of cortical cell division during root nodule development in Lotus japonicus is accompanied by auxin response. Dev **139**: 3997–4006

Tian H, Wabnik K, Niu T, Li H, Yu Q, Pollmann S, Vanneste S, Govaerts W, Rolčík J, Geisler M, et al (2014) WOX5-IAA17 feedback circuit-mediated cellular auxin response is crucial for the patterning of root stem cell niches in arabidopsis. Mol Plant **7**: 277–289

Tirichine L, Sandal N, Madsen LH, Radutoiu S, Albrektsen AS, Sato S, Asamizu E, Tabata S, Stougaard J (2007) A gain-of-function mutation in a cytokinin receptor triggers spontaneous root nodule organogenesis. Science (80-) **315**: 104–107

To JPC, Deruère J, Maxwell BB, Morris VF, Hutchison CE, Ferreira FJ, Schaller GE, Kieber JJ (2007) Cytokinin regulates type-A Arabidopsis response regulator activity and protein stability via two-component phosphorelay. Plant Cell **19**: 3901–3914

Wahl V, Brand LH, Guo YL, Schmid M (2010) The FANTASTIC FOUR proteins influence shoot meristem size in Arabidopsis thaliana. BMC Plant Biol. doi: 10.1186/1471-2229-10-285

Wingler A, Fritzius T, Wiemken A, Boller T, Aeschbacher RA (2000) Trehalose induces the ADP-glucose pyrophosphorylase gene, ApL3, and starch synthesis in Arabidopsis. Plant Physiol **124**: 105–114

Xuelin Wu, Tsagaye Dabi DW (2005) Requirement of Homeobox Gene STIMPY/WOX9 for Arabidopsis Meristem Growth and Maintenance. Curr Biol **15**: 436–440

Van Zeijl A, Op Den Camp RHM, Deinum EE, Charnikhova T, Franssen H, Op Den Camp HJM, Bouwmeester H, Kohlen W, Bisseling T, Geurts R (2015) Rhizobium Lipo-chitooligosaccharide Signaling Triggers Accumulation of Cytokinins in Medicago truncatula Roots. Mol Plant **8**: 1213–1226

Zhao Y, Hu Y, Dai M, Huang L, Zhou DX (2009) The WUSCHEL-Related homeobox gene WOX11 is required to activate shoot-borne crown root development in rice. Plant Cell **21**: 736–748

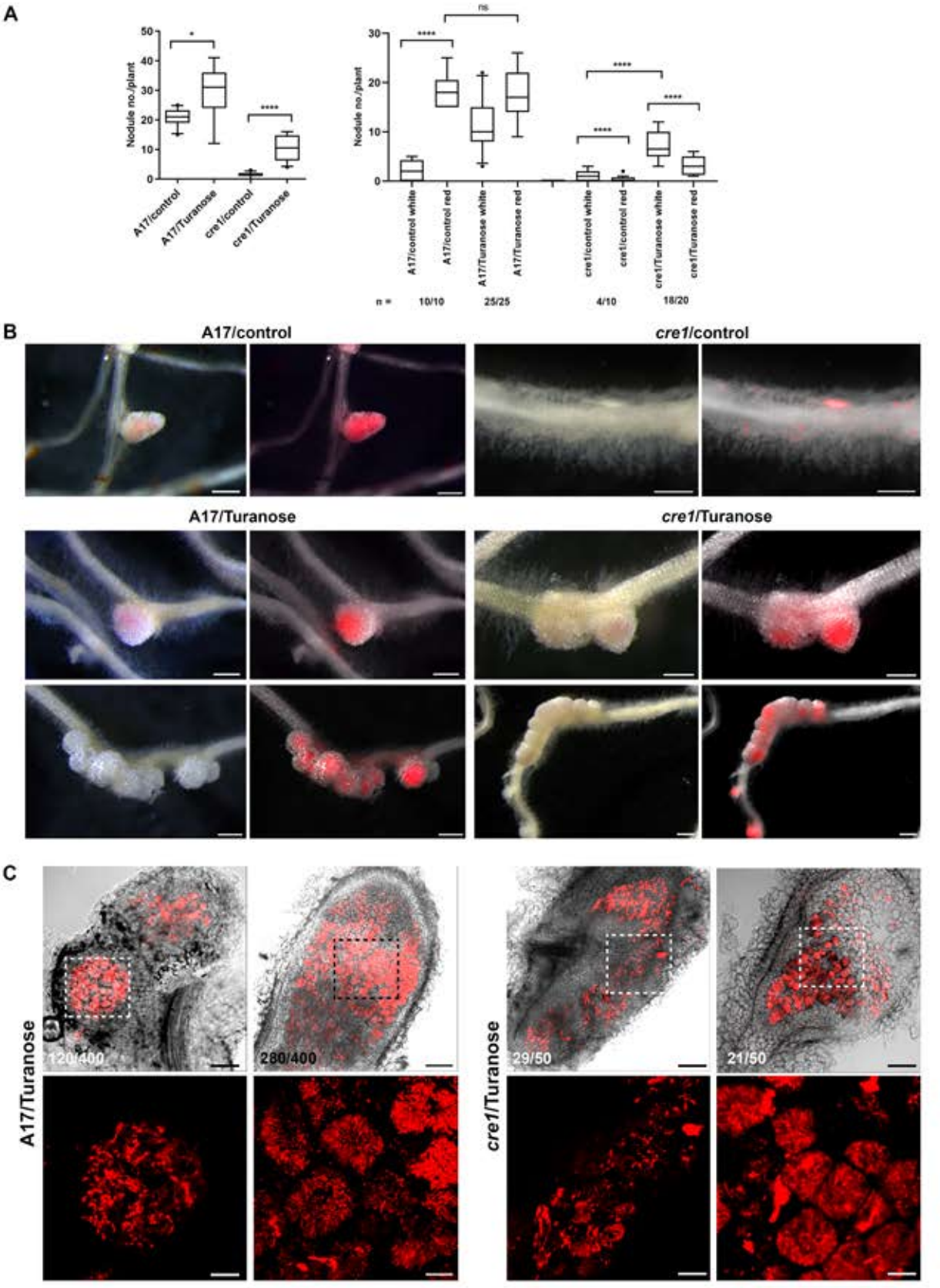

Figure 1: Complementation of nodulation in *cre1* mutants using non-metabolizable sucrose analogue Turanose. (A) Box plot represents nodule number per plant where histogram represent mean ± SD. Separate plots indicates cumulative and red/white nodules 3-4 weeks after infection (WAI) with *Sinorhizobium meliloti Sm2011-pBHR-mRFP* under control and 10^{-3}M turanose treatment. Student's t-test was used to assess significant differences, where **** and * indicate P<0.0001 and <0.01 respectively, n indicates the number of roots systems with infection events per total number of scored roots.
(B) Morphology of nodules in A17 and *cre1* mutants 3-4WAI. Representative micrograph of control and turanose treated roots indicated as bright field and bright field+ mRFP merged.
(C) Ultrastructure analysis of nodules in A17 and *cre1* after turanose treatment, where the perforated box represents the infection zone with its corresponding enlarged view below the respective images. Total number of each type of nodules observed out of the total observed nodules are indicated at the left-hand corner. (upper panel) Brightfield + mRFP merged and (lower panel) mRFP. Scale bar: B= 500µm, C (upper panel) = 100µm and (lower panel) = 10µm.

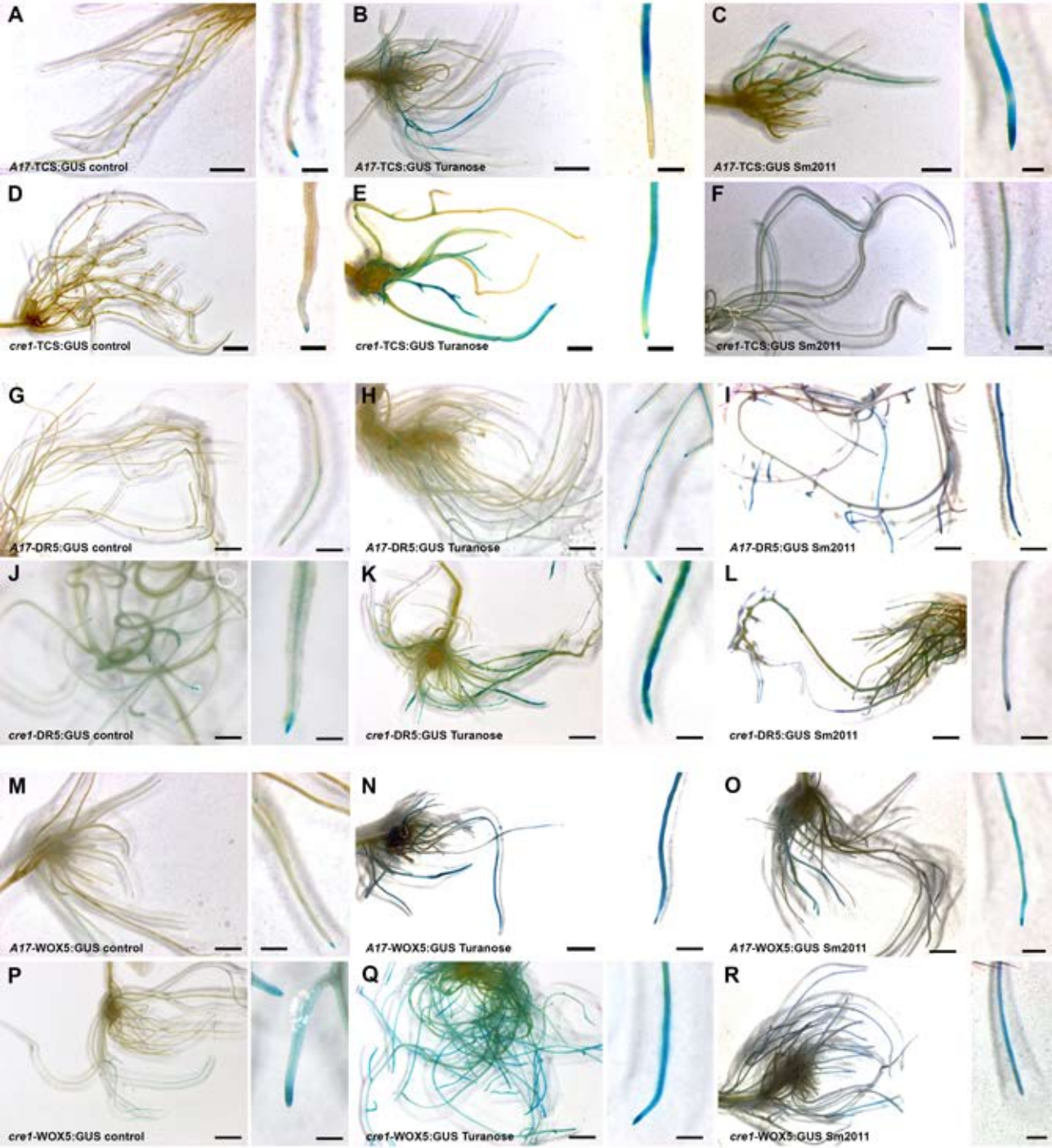

Figure 2: Turanose treatment and infection with *Sm2011-pBHR-mRFP* differentially induces cytokinin (*pTCS:GUS*), auxin (*pDR5:GUS*) and WOX5 (*pWOX5:GUS*) expression in A17 and *cre1* mutants. (A-F) *pTCS:GUS* expression in (A-C) A17 roots under control (A), 10^{-3}M Turanose treatment (B) and after *Sm2011* infection (C); (D-F) *cre1* roots under control (D), 10^{-3}M Turanose treatment (E) and after *Sm2011* infection (F).
(G-L) *pDR5:GUS* expression in (G-I) A17 roots under control (G), 10^{-3}M Turanose treatment (H) and after *Sm2011* infection (I); (J-L) *cre1* roots under control (J), 10^{-3}M Turanose treatment (K) and after *Sm2011* infection (L).
(M-R) *pWOX5:GUS* expression in (M-O) A17 roots under control (M), 10^{-3}M Turanose treatment (N) and after *Sm2011* infection (O); in (P-R) *cre1* roots under control (P), 10^{-3}M Turanose treatment (Q) and after *Sm2011* infection.
Root were harvested 1 week post treatment with turanose and 1 week after infection with *Sm2011-pBHR-mRFP*. At least 20 individual samples were observed for each treatment and representative images are presented. Scale bar = 5mm (whole root) and 2mm (single root).

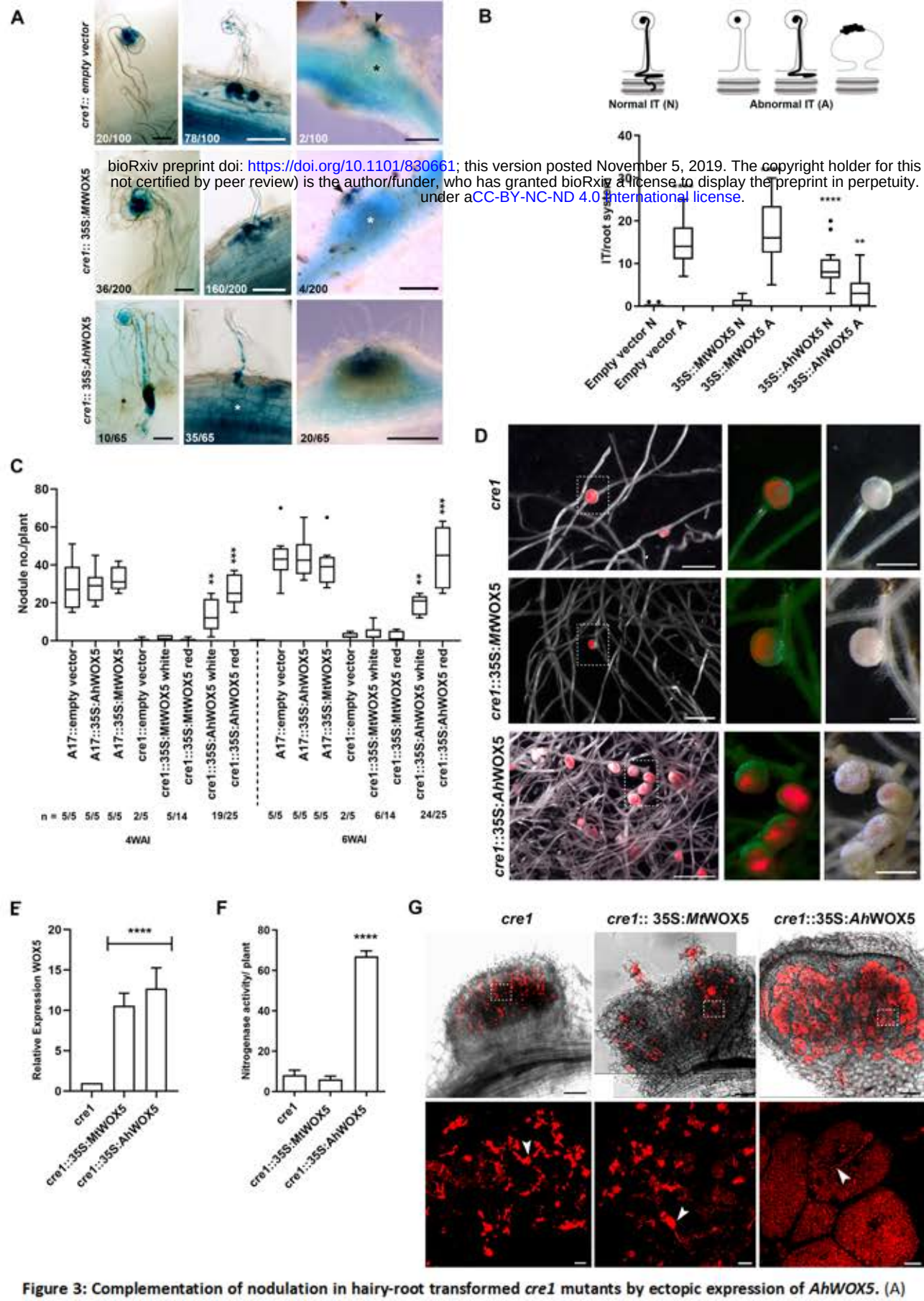

Figure 3: Complementation of nodulation in hairy-root transformed *cre1* mutants by ectopic expression of *AhWOX5*. (A) Epidermal infection thread (IT) observed under bright field microscope 2WAI with *Sm1021-pXLGD4-lacZ* in *cre1* roots transformed with empty vector, *p35S:eGFP-MtWOX5* and *p35S:eGFP-AhWOX5*. Total number of each type of infection threads (IT) observed out of the total number of early infection events are indicated at the left-hand corner. Scale bar = 100µm.

Box plot represents (B) IT/ root system and (C) Nodule number/ root system where histogram represent mean ± SD. Student's t-test was used to assess significant differences, where **** and ** indicates P<0.0001 and P<0.004 respectively and n indicates the number of roots systems with infection events per total number of scored roots.

(D) Morphology of nodules in transgenic hairy-roots of *cre1*mutant 4WAI with *Sm2011-pBHR-mRFP*. Representative micrograph of transgenic roots indicated as bright field+ mRFP merged and inset as eGFP+ mRFP merged and bright field. Scale bar = 1mm and inset = 500µm.

(E) qRT-PCR analysis of *MtWOX5* and *AhWOX5* relative to control transformed (*cre1*) roots normalised against *MtActin*. (F) Acetylene reduction assay (nmole C_2H_4/h/mg nodule) in indicated root system. For E and F, Histogram represents an average of three biological replicates each having n>4 plants and error bar represents SD. Student's t- test was used to assess significant differences, where **** indicate P<0.0001.

(G) Ultrastructure of nodules developed in *cre1* mutant transformed with different constructs where the perforated box represents the infection zone with its corresponding enlarged view below the respective images. Scale bar: G (upper panel) = 100µm and (lower panel) = 10µm. Arrow indicate infection thread and * indicate cell division.

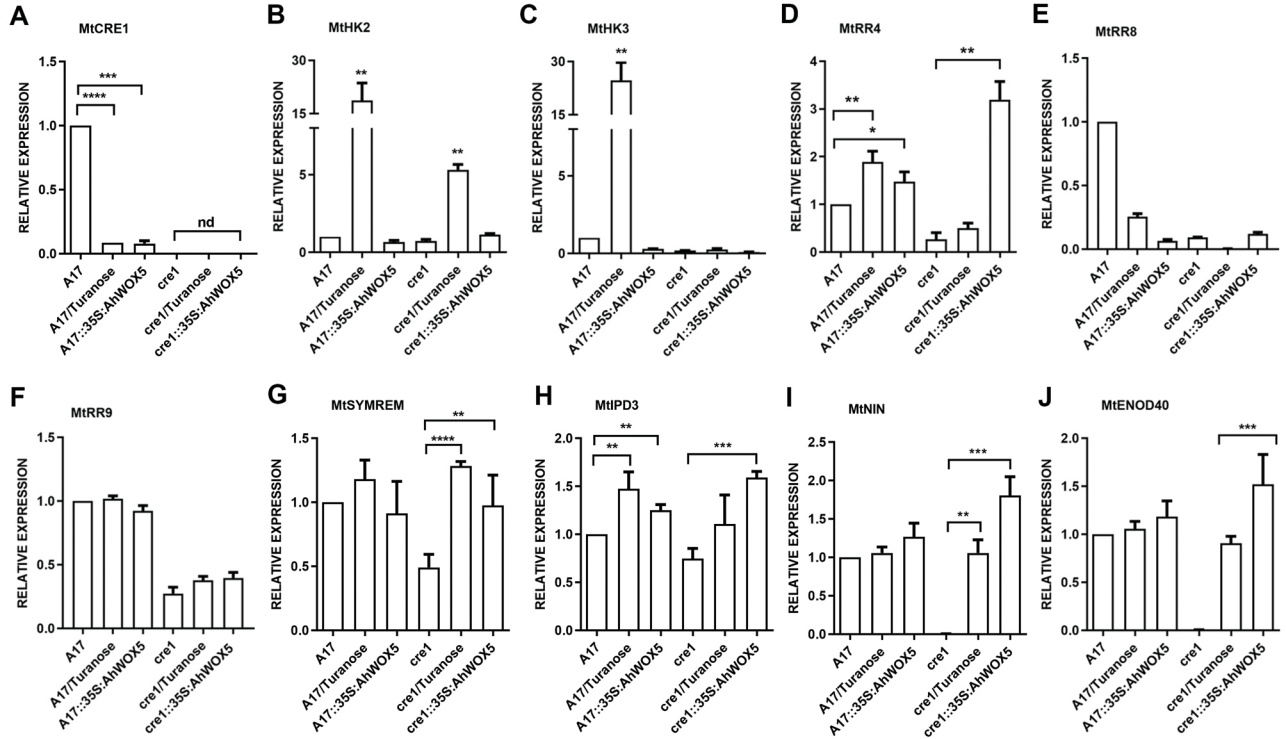

Figure 4: Differential recruitment of cytokinin signalling and sym pathway during the complementation of *cre1* mutant under turanose treatment and *AhWOX5* ectopic expression. qRT-PCR analysis of *MtCRE1* (A), *MtHK2* (B), *MtHK3* (C), *MtRR4* (D), *MtRR8* (E) *MtRR9* (F) *MtSYMREM* (G), *MtIPD3* (H), *MtNIN* (I) and *MtENOD40* (J) 4WAI with *Sm2011-pBHR-mRFP* in roots of A17, A17/Turanose, A17::35S:*AhWOX5*, *cre1*, *cre1*/Turanose and *cre1*::35S:*AhWOX5* relative to A17. *MtActin* was used as a reference gene. Histogram represents an average of three biological replicates each having n>4 plants and error bar represents SD. Student's t-test was used to assess significant differences where ****, ***, ** and * indicate P<0.0001, 0.0001, 0.005 and 0.04 respectively.

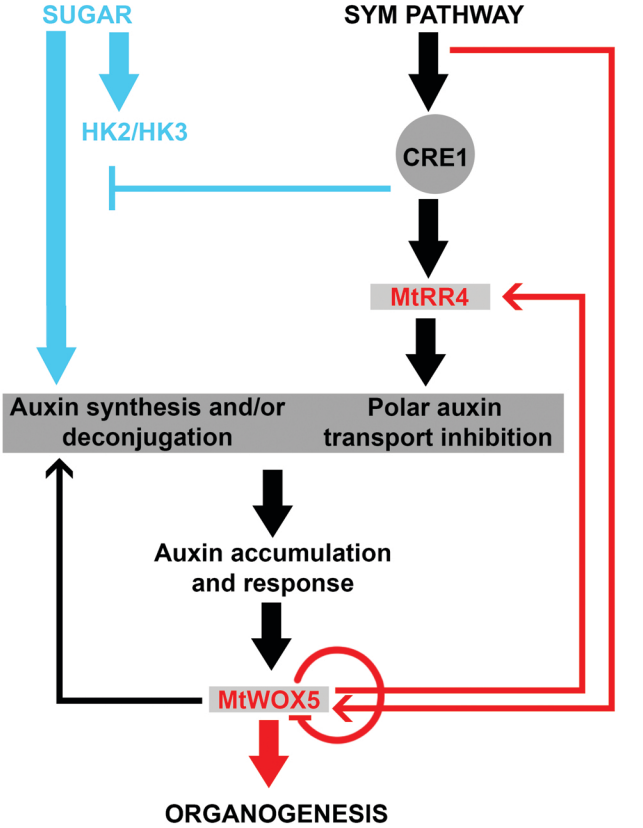

Figure 5: Proposed Model for the role of sugar signalling and WOX5 expression in restoration of symbiotic efficiency in *M. truncatula* cytokinin perception mutant *cre1*. Black arrows indicate the known sym pathway dependent CRE1 activation that leads to auxin accumulation and WOX5 induction to generate the nodule primordia. We propose sugar signalling to restore symbiosis in *cre1* by (i) redundant action of MtHK2 that compensates MtCRE1 and by (ii) directly triggering auxin responses that is inhibited by CRE1 (Blue arrows). WOX5 restore symbiosis in cre1 by induction of (i) *MtRR4* a response regulator required for symbiosis and by directly triggering auxin responses). WOX5 is activated by SYM pathway and its function is governed by post transcriptional homeostatic controls (Red arrows). Forward arrow indicates activation and blunt arrow indicates inactivation.